pathogens

MDPI

Article

Genomic Surveillance of Infectious Bursal Disease Virus in Brazil Identifies a Novel Genogroup B6 and Putative Reassortment Events

Jorge Luis Chacón [1], Cesar Nunes [1], Brunno Fernandes [1], Branko Alva [1], Ruy D. Chacón [2,*] and Antonio J. Piantino Ferreira [2,*]

[1] Veterinary Services, Ceva Animal Health, São Paulo 13148-115, Brazil; jorge.chacon@ceva.com (J.L.C.); cesar.nunes@ceva.com (C.N.); brunno.ferreira@ceva.com (B.F.); branko.alva@ceva.com (B.A.)
[2] Department of Pathology, School of Veterinary Medicine, University of São Paulo, São Paulo 05508-270, Brazil
* Correspondence: ruychaconv@alumni.usp.br (R.D.C.); ajpferr@usp.br (A.J.P.F.)

Abstract

Infectious bursal disease virus (IBDV) is a major immunosuppressive pathogen of poultry that can compromise immune function and increase susceptibility to secondary infections; however, its segment-level genomic diversity in Brazil remains insufficiently characterized. We conducted an integrated molecular surveillance study combining diagnostic detection, VP2 and VP1 sequencing, phylogenetic and genomic constellation analyses, selection analyses, and recombination screening. IBDV was detected in 88 clinical samples among suspected flocks (85.4%), with detection increasing markedly after 14 days of age. Among 21 samples selected for sequencing, 17 VP2 sequences were classified as A4, while 15 VP1 sequences belonged to B1 or the novel B6 genogroup. Among samples with paired VP2–VP1 data, A4B1 was identified in 10/11 samples and A4B6 in one. Analysis of these sequences together with historical Brazilian sequences with paired segments identified A3B2 and A4B1 as the predominant genomic constellations, with A3B2 detected from 2001 to 2024 and A4B1 from 1983 to 2025. Notably, three VP1 sequences were classified within B6, which occurred in both A3 and A4 backgrounds, generating A3B6 and A4B6 constellations consistent with putative reassortment. VP2 exhibited localized diversification against a background of predominant purifying selection, including sites under episodic diversifying selection within the exposed P_{BC}, P_{DE}, and P_{HI} loops. Together, these findings reveal a more dynamic genomic landscape of Brazilian IBDV than suggested by VP2-based surveillance alone, with novel B6-associated constellations providing evidence of previously unrecognized segment-level diversity and putative reassortment, underscoring the importance of dual-segment genomic surveillance for monitoring IBDV evolution and adapting prevention protocols in Brazil.

Keywords: *Avibirnavirus gumboroense*; segment A; segment B; VP2; VP1; hypervariable region; genomic constellations; A4B1; A3B2; reassortant

Academic Editor: Mario Forzan

Received: 30 September 2026
Revised: 30 October 2026
Accepted: 2 November 2026
Published: 3 November 2026

Copyright: © 2026 by the authors. Licensee MDPI, Basel, Switzerland. This article is an open access article distributed under the terms and conditions of the Creative Commons Attribution (CC BY) license.

1. Introduction

Infectious Bursal Disease Virus (IBDV), classified within the species *Avibirnavirus gumboroense* in the family *Birnaviridae*, stands out as one of the most economically and

epidemiologically impactful immunosuppressive agents in the worldwide poultry industry [1]. IBDV preferentially targets and depletes differentiating B lymphocytes within the bursa of Fabricius in young chickens, triggering a clinical course that ranges from acute forms with high mortality to subclinical infections characterized by severe immunosuppression. The latter condition can substantially compromise immune responses to routine vaccinations and increase susceptibility to secondary viral and bacterial infections, potentially resulting in increased mortality, impaired flock performance, and production losses [2,3].

The IBDV genome is bisegmented and consists of two molecules of double-stranded RNA (dsRNA), designated as Segment A and Segment B. Segment A, which is approximately 3.2 kb in length, contains two partially overlapping open reading frames (ORFs). The smaller ORF encodes the non-structural protein VP5, which is involved in cellular apoptosis regulation and viral pathogenesis. The larger ORF encodes a polyprotein (VP2–VP4–VP3) that undergoes autocatalytic processing by the viral protease VP4 to generate the mature structural proteins VP2 and VP3 [4–6]. The VP2 protein constitutes the outer surface of the viral capsid and is the primary antigenic determinant of the virus, hosting the hypervariable region (hvVP2). Structurally, this region is formed by loops exposed to the exterior (loops BC, DE, FG, and HI), which contain residues involved in viral infectivity, antigenic recognition, and neutralization by protective antibodies [7]. Conversely, Segment B, approximately 2.8 kb in length, encodes the VP1 protein, an RNA-dependent RNA polymerase (RdRp) responsible for genomic replication and transcription. Although traditionally considered a secondary component in molecular studies, VP1 has taken on a leading role after demonstrations that it interacts directly with Segment A proteins, contributing to viral replication efficiency and the modulation of viral pathogenicity and virulence [8,9].

The genetic evolution of IBDV is driven primarily by point mutations and genomic reassortment, while homologous recombination within individual genomic segments has also been reported but appears to occur less frequently [10–12]. As an RNA virus lacking a conventional proofreading mechanism, IBDV is prone to replication errors that contribute to genetic diversification. The accumulation of amino acid substitutions within the hvVP2 region can contribute to antigenic variation and may facilitate immune escape from VP2-based vaccination [13,14]. Furthermore, genomic reassortment can occur when two genetically distinct IBDV strains co-infect the same host, generating viruses with novel combinations of Segment A and Segment B and potentially altering viral phenotypes, including pathotypes [10,15–18]. Although historically reported as less frequent, homologous recombination has also been described in IBDV and may generate mosaic sequence patterns within individual genomic segments [11,12].

To organize this growing genetic diversity, epidemiological classification has transitioned from classical phenotypic schemes toward objective molecular models. Historically, IBDV strains have been categorized into classical virulent (cvIBDV), very virulent (vvIBDV), antigenic variant (avIBDV), and distinct IBDV (dIBDV) groups, with dIBDV strains initially described predominantly in South American populations [1,19–22]. However, current molecular phylogeny classification systems offer a more comprehensive and independent genotypic structuring for both genomic segments. Under this model, Segment A is divided into eight genogroups (A1–A8), whereas Segment B comprises five genogroups (B1–B5) [22,23]. This dual-segment nomenclature (AxBx) is particularly useful for identifying genomic reassortment events that may influence viral pathogenicity and remain undetected when molecular surveillance is restricted to Segment A alone.

In the geographical context of South America, and particularly in Brazil, one of the largest producers and exporters of poultry meat globally, the epidemiological situation of IBDV has not been fully clarified under dual-segment characterization. Despite the

relevance of this problem, the vast majority of molecular surveillance and IBDV characterization efforts in Brazil have focused almost exclusively on the partial sequencing of the VP2 protein gene (Segment A) [24–27]. As a result, the diversity and distribution of Segment-B (VP1) lineages and their relationships with Segment-A lineages remain insufficiently characterized, making it difficult to determine the extent of reassortment and other genomic patterns contributing to the diversification of IBDV in Brazil. The lack of paired genomic information for both segments therefore represents an important knowledge gap for understanding the segment-specific evolutionary dynamics, genomic constellations, and persistence of IBDV in the country, with potential implications for the interpretation of molecular surveillance and the development of regionally informed diagnostic and control strategies.

To address this gap, the present study aimed to comprehensively characterize IBDV strains circulating in Brazil through systematic analysis of both genomic segments (A and B). We integrated molecular diagnosis with phylogenetic and evolutionary bioinformatics approaches to evaluate the viral detection rate in commercial farms, reconstruct its phylogenetic history, characterize genomic constellations, and perform exploratory analyses of diversifying selection and homologous recombination. We further examined amino acid polymorphisms within the exposed regions of the VP2 capsid protein. By integrating segment-specific characterization with evolutionary and genomic analyses, this study provides updated evidence on the diversity and evolutionary dynamics of IBDV in Brazil and clarifies the contribution of segment-specific variation and genomic reassortment to the diversification of circulating strains in the Brazilian poultry industry.

2. Materials and Methods

2.1. Clinical Samples

This study included 103 pooled Bursa of Fabricius samples per flock submitted to the Laboratory of Avian Diseases, School of Veterinary Medicine, University of São Paulo, Brazil, due to suspected infectious bursal disease virus (IBDV) infection and/or clinical signs consistent with immunosuppression. Thus, samples were obtained from commercial flocks experiencing recurrent low productivity and/or sanitary disturbances. Vaccination history was available for all sampled birds. The reported vaccination categories included immune-complex vaccines, live attenuated vaccines, recombinant HVT-IBD vaccines, and vaccinated birds for which the vaccine type was unspecified (Table S1). The 103 clinical samples analyzed in this study were collected over an 18-month period, from January 2025 to June 2026, and originated from nine Brazilian states. All samples represented independent commercial farms and consisted predominantly of broilers (n = 79) and layers (n = 23), with one sample originating from a broiler breeder flock (n = 1). The age of the birds at sampling ranged from 1 day to 30 weeks, depending on the production type.

Each sample consisted of a pool of three to five bursae collected from birds belonging to the same commercial farm. The bursae were collected and immediately frozen at −20 °C until laboratory processing. For molecular analyses, pooled bursae were mechanically macerated using sterile scissors and homogenized in phosphate-buffered saline (PBS) at a 1:1 tissue-to-buffer ratio (w/v), with the final homogenate adjusted to a volume of 1.5 mL. The resulting homogenates were subsequently used for nucleic acid extraction and molecular detection of IBDV.

2.2. Nucleic Acids Extraction and IBDV Detection

Homogenized Bursa of Fabricius samples were subjected to three freeze–thaw cycles, consisting of freezing at −80 °C for 10 min followed by thawing at 56 °C for 1 min. Samples were subsequently centrifuged at 12,000× g for 20 min at 4 °C, and 200 µL of the clarified

supernatant was used for total nucleic acid extraction. Viral nucleic acids were extracted using the ReliaPrep™ Viral TNA Miniprep System Kit (Promega, Madison, WI, USA) according to the manufacturer's instructions. Extracted nucleic acids were quantified using a NanoDrop One spectrophotometer (Thermo Scientific™, Wilmington, DE, USA) and stored at −20 °C until further analysis.

Complementary DNA (cDNA) was synthesized by reverse transcription using the M-MLV Reverse Transcriptase kit (Life Technologies, Carlsbad, CA, USA) and random hexamer primers (Invitrogen), following the manufacturer's instructions.

IBDV was detected by quantitative polymerase chain reaction (qPCR) targeting a 111-bp fragment of Segment A. The assay was adapted from the protocol described by Techera et al. (2019) [28] for SYBR® Green-based detection. Amplification was performed using primers F143 (5′-CMAGATCAAACCCAACAGATTGT-3′) and R253 (5′-CTCTGACCTGAGAGTGTGCTTCTC-3′) with PowerUp™ SYBR® Green Master Mix (Applied Biosystems, Austin, TX, USA) on a QuantStudio™ 3 Real-Time PCR System (Applied Biosystems, Marsiling, Singapore). SYBR® Green amplification was assessed by melting-curve analysis to verify the presence of a single specific amplification product. Samples with Ct < 28 were preferentially selected for sequencing because lower Ct values were expected to provide sufficient template for successful amplification of the longer VP2 and VP1 targets.

2.3. Sequence and Phylogenetic Analysis

Molecular typing was performed by sequencing genomic Segments A and B. For Segment A, the hypervariable region of the VP2 gene was amplified using primers INCO-DC#3F (5′-AACAGCCAACATCAACG-3′) and INCO-DC#4R (5′-GCTCGAAGTTGCTCACCC-3′). PCR amplification and thermocycling conditions were performed as previously described [22,29,30], generating a 677-bp amplicon corresponding to nucleotides 571–1247 of the VP2 gene. For Segment B, the VP1 gene was amplified using primers B-Univ-F (5′-AATGAGGAGTATGAGACCGA-3′) and B-Univ-R (5′-CCTTCTCTAGGTCAATTGAGTACC-3′). PCR amplification and thermocycling conditions followed a previously described protocol [31], generating a 1051-bp amplicon spanning nucleotides 319–1369 of the VP1 gene.

PCR products were sequenced bidirectionally using the Sanger method on a 3500xL Genetic Analyzer with the BigDye™ Terminator v3.1 Cycle Sequencing Kit (Applied Biosystems, Foster City, CA, USA). Electropherograms were inspected, assembled, and trimmed using Geneious Prime® v2026.1.2.

For phylogenetic analyses, separate VP1 and VP2 datasets were constructed. Reference sequences were retrieved from GenBank based on the representative IBDV strains included by Islam et al. (2021) [22], comprising 86 VP1 and 101 VP2 sequences. These datasets were supplemented with additional Brazilian, Argentinian, and Uruguayan sequences (52 strains for which both VP1 and VP2 sequences were available), including previously characterized Brazilian strains, and sequences generated in the present study (15 VP1 and 17 VP2 sequences). In addition, Reference sequences representing the vaccine strains Faragher 52/70, Winterfield 2512, D78, V877, and MB were retrieved from GenBank. Their accession numbers are provided in their respective figures. Thus, the final datasets comprised 157 VP1 and 176 VP2 sequences, respectively. Phylogenetic analyses were restricted to the homologous regions shared with reference sequences, yielding alignments of 366 bp for VP2 and 508 bp for VP1 [22].

Sequence alignments were generated using MAFFT Online v7.526 [32]. For each dataset, the best-fitting nucleotide substitution model was selected using the Bayesian Information Criterion (BIC) implemented in PhyML v3.3 [33]. Maximum-likelihood phylogenetic trees were subsequently reconstructed in PhyML v3.3 using the selected

substitution model. Branch support was assessed using the approximate likelihood-ratio test with the Shimodaira–Hasegawa-like (aLRT SH-like) method, a fast branch-support approach implemented in PhyML. The resulting trees were visualized and edited using iTOL v7 [34].

Pairwise nucleotide and deduced amino acid identity matrices were generated for all sequences included in the respective datasets to assess overall sequence similarity. In addition, polymorphic sites were identified from the multiple sequence alignments and compared between the genogroup(s) containing Brazilian strains and the remaining reference genogroups. This analysis was used to identify nucleotide and amino acid positions that may contribute to genetic differentiation among the major IBDV genogroups.

To further assess genetic divergence among VP1 and VP2 genogroups, average evolutionary distances between the identified genogroups were estimated in MEGA v12 using the Maximum Composite Likelihood model [35,36]. Rate variation among sites was modelled using a gamma distribution with a shape parameter of 1.0. Pairwise deletion was applied for the treatment of gaps and missing data and mean evolutionary distances between genogroups were calculated using the between-group average option.

2.4. Selective Pressure and Recombination Analyses

Selective pressure and recombination analyses were performed on an exploratory basis. For selective pressure analyses, the analysis was restricted to VP2 of the genogroups with the largest representation of Brazilian strains (A3 and A4), including both previously available Brazilian sequences and sequences generated in the present study. All available sequences belonging to the selected genogroups were included, regardless of geographic origin, to provide a broader representation of their genetic diversity.

Episodic diversifying selection was assessed using the Mixed Effects Model of Evolution (MEME), with a significance threshold of $p < 0.1$, consistent with author recommendations [37]. Site-specific pervasive selection was evaluated using the Fixed Effects Likelihood (FEL) method, also applying a significance threshold of $p < 0.1$, consistent with author recommendations [38].

Exploratory recombination analysis was performed using RDP5 [39], applying the RDP, GENECONV, BootScan, MaxChi, Chimaera, SiScan, and 3Seq algorithms. Because only partial VP2 and VP1 fragments were available, recombination analyses were interpreted as exploratory and restricted to the analyzed regions. For conservative interpretation, putative recombination events were considered credible only when supported by at least five independent detection methods.

2.5. Statistical Analysis

Descriptive statistics were used to summarize IBDV detection according to production type, geographic region, and bird age. Detection rates were calculated as the proportion of positive samples among the total number of samples in each category, and the overall detection rate was reported with a 95% confidence interval calculated using the Wilson method. Differences in IBDV detection between broilers and layers were assessed using Fisher's exact test. Differences in detection among age categories were evaluated using the Fisher–Freeman–Halton exact test. Birds were stratified into four age categories (≤14, 15–28, 29–42, and >42 days) using consecutive 14-day intervals to facilitate descriptive comparisons across the broiler production cycle. The first cutoff also has biological relevance because maternally derived antibodies against IBDV decline during early life, while the timing of vaccine-virus replication and the development of vaccine-induced immunity depend on the vaccination platform and maternal antibody levels. Bird age was compared between IBDV-positive and negative samples using the Mann–

Whitney U test, both for the overall dataset and separately among broilers and layers. Statistical significance was set at $p < 0.05$. All statistical analyses were performed in R version 4.6.1.

3. Results

3.1. IBDV Detection in Clinical Samples

IBDV was detected in 88 of the 103 clinical samples analyzed, corresponding to an overall detection rate of 85.4% (95% CI: 77.4–91.0%). The 103 samples originated from nine Brazilian states and represented three production types: broilers, layers, and broiler breeders.

3.1.1. IBDV Detection According to Production Type

IBDV was detected in 69 out of 79 broiler samples (87.3%) and 19 out of 23 layer samples (82.6%), whereas the single broiler breeder sample was negative (Table 1). Detection rates did not differ significantly between broilers and layers (Fisher's exact test, $p = 0.513$).

Table 1. IBDV detection according to production type.

Production Type	*n*	Positive, *n* (%)	Negative, *n* (%)
Broiler	79	69 (87.3)	10 (12.7)
Layer	23	19 (82.6)	4 (17.4)
Broiler breeder [1]	1	0 (0.0)	1 (100.0)
Total	103	88 (85.4)	15 (14.6)

[1] Broiler breeders were not included in Fisher's exact test comparisons due to their limited sample size.

3.1.2. Geographic Distribution of IBDV Detection

IBDV-positive samples were identified in eight of the nine states represented in the dataset. The highest numbers of samples originated from São Paulo ($n = 43$), Pernambuco ($n = 19$), and Paraná ($n = 15$). Detection rates varied among states, ranging from 25.0% in Mato Grosso (1/4) to 100% in Rio Grande do Sul (6/6), Rondônia (6/6), and Espírito Santo (1/1). Because the number of samples contributed by individual states varied substantially, these state-specific detection rates should be interpreted descriptively rather than as estimates of geographic prevalence. Accordingly, no formal statistical comparisons among states were performed. The complete state-level distribution is provided in Table S1 and is illustrated geographically in Figure S1.

3.1.3. IBDV Detection According to Bird Age

Bird age at sampling ranged from 1 to 210 days. Among IBDV-positive samples, the median age was 28 days (IQR: 27–34.3), whereas negative samples had a median age of 24 days (IQR: 14–28). The overall age distributions differed significantly between IBDV-positive and negative samples (Mann–Whitney U test, U = 942.0, $p = 0.0081$). Positive samples were predominantly obtained from young birds, with ages ranging from 1 to 91 days, whereas negative samples included birds up to 210 days of age.

To further characterize IBDV detection across age groups, samples were classified into four age categories (Table 2). The observed detection rate was 37.5% (3/8; 95% CI: 8.5–75.5%) among birds ≤14 days old, compared with 88.5% (46/52; 95% CI: 76.6–95.6%) among birds aged 15–28 days, 92.9% (26/28; 95% CI: 76.5–99.1%) among birds aged 29–42 days, and 86.7% (13/15; 95% CI: 59.5–98.3%) among birds >42 days. The estimate for birds ≤14 days was imprecise because of the small sample size. Detection rates differed across age categories (Fisher–Freeman–Halton exact test, $p = 0.0019$).

Table 2. IBDV detection according to age category.

Age Category [1]	*n*	Positive, *n* (%)	Negative, *n* (%)	95% CI
≤14 days	8	3 (37.5)	5 (62.5)	8.5–75.5%
15–28 days	52	46 (88.5)	6 (11.5)	76.6–95.6%
29–42 days	28	26 (92.9)	2 (7.1)	76.5–99.1%
>42 days	15	13 (86.7)	2 (13.3)	59.5–98.3%
Total	103	88 (85.4)	15 (14.6)	

[1] Comparison across all age categories: Fisher–Freeman–Halton exact test, $p = 0.0019$. Values are presented as positive/number tested (%). The 95% confidence intervals (CIs) were calculated using the exact binomial Clopper–Pearson method.

3.1.4. Age Distribution According to Production Type and IBDV Detection

Because bird age was strongly associated with production type, age distributions were further examined separately among broilers and layers. Among broilers, IBDV-positive samples had a median age of 28 days (IQR: 27–34 days), compared with 25.5 days (IQR: 12–27 days) among negative samples; this difference was statistically significant (Mann–Whitney U test, U = 518.5, $p = 0.0099$). In contrast, among layers, positive samples had a median age of 49 days (IQR: 28–84 days), compared with 17.5 days (IQR: 14–175 days) among negative samples, although this difference was not statistically significant (U = 52.5, $p = 0.253$). The age distributions according to production type and IBDV detection status are shown in Figure 1, with the corresponding descriptive statistics summarized in Table 3.

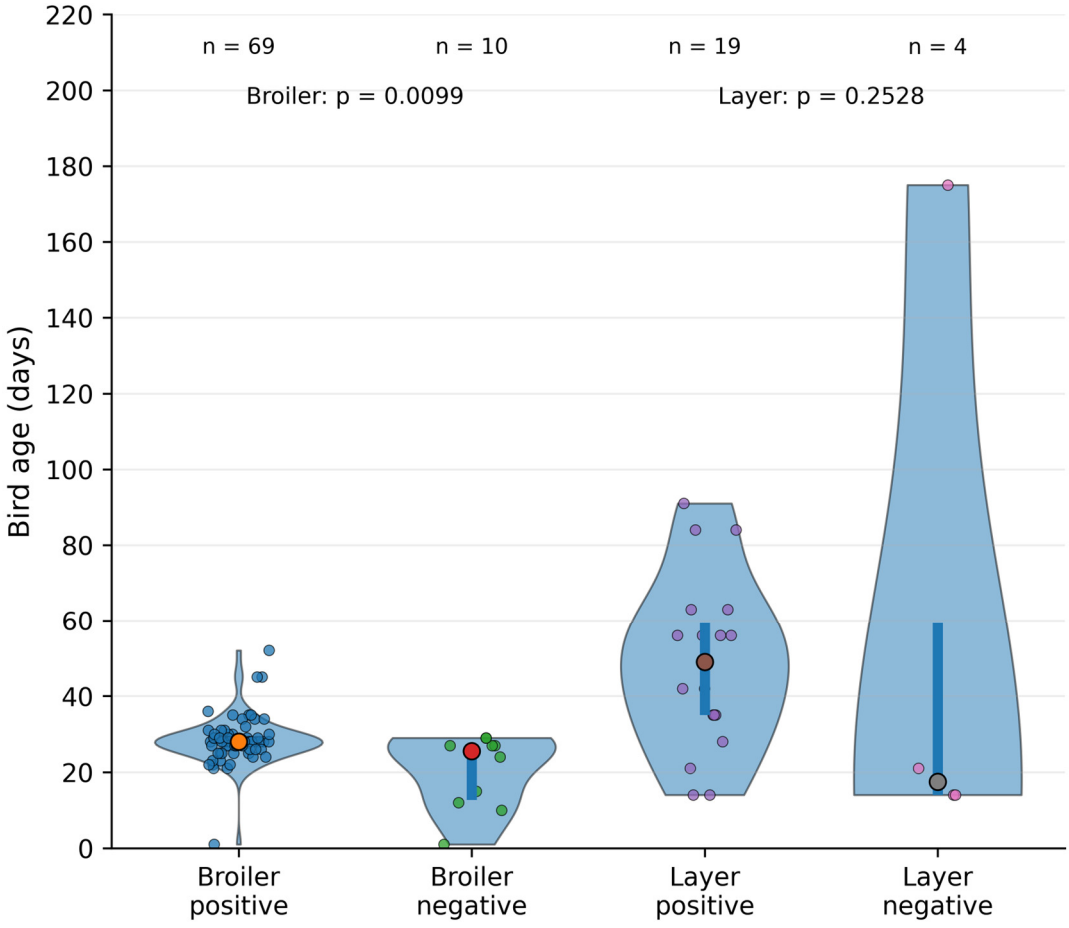


Figure 1. Age distribution according to production type and IBDV detection. Age distribution of clinical samples stratified by production type and IBDV detection status. Violin plots show the distribution of bird age, with individual points representing individual samples. The central marker

indicates the median and the vertical line the interquartile range (IQR). Comparisons between IBDV-positive and IBDV-negative samples were performed separately for broilers and layers using the Mann–Whitney U test. A significant difference in age distribution was observed among broilers ($p = 0.0099$), whereas no significant difference was detected among layers ($p = 0.2528$). The breeder group was not included in the stratified comparison because only one sample was available.

Table 3. Age distribution of IBDV-positive and negative samples according to production type.

Production Type [1]	IBDV Status	*n*	Median Age (Days)	IQR (Days)	Range (Days)	*p*-Value
Broiler	Positive	69	28	27–34	1–52	0.0099
	Negative	10	25.5	12–27	1–29	
Layer	Positive	19	49	28–84	14–91	0.2528
	Negative	4	17.5	14–175	14–175	

[1] Age comparison by IBDV detection status within production type: Mann–Whitney U test; broilers, $p = 0.0099$; layers, $p = 0.253$.

3.2. Sequence and Phylogenetic Analysis

Maximum-likelihood analysis of the VP2 dataset resolved the Brazilian and reference sequences into the previously established Segment A genogroups A0–A8 (Figure 2). Brazilian sequences were identified within A1a, A1b, A3, and A4. The A3 genogroup (traditionally associated with the very virulent, vvIBDV pathotype) showed a broad geographic distribution, including sequences from Brazil and multiple other countries. Brazilian sequences were interspersed among sequences from different geographic origins rather than forming a single geographically restricted cluster. In contrast, A4 genogroup (formerly, distinct, dIBDV), showed a more pronounced geographic structure, with Brazilian sequences forming closely related clusters that were different from sequences from Uruguay and Argentina. Notably, all 17 VP2 sequences generated in the present study clustered within A4, indicating a consistent association of the newly characterized Brazilian viruses with this genogroup. A4 has historically been strongly associated with South America, and the present phylogeny indicates that this geographic association has persisted over time, with historical Brazilian sequences distributed within the same lineage and the recently generated sequences remaining within A4. The presence of multiple Brazilian A4 sequences spanning different sampling periods, including the most recent sequences generated in this study, is consistent with the continued circulation of A4-associated viruses in Brazil. Despite this geographic pattern, no distinct subclusters associated with geographic region, production type, or sampling year were identified among the Brazilian A4 sequences. Overall, the VP2 phylogeny revealed contrasting geographic patterns between the major Brazilian-associated genogroups, with A3 exhibiting a broad geographic distribution and A4 maintaining a more pronounced South American, particularly Brazilian, clustering pattern.

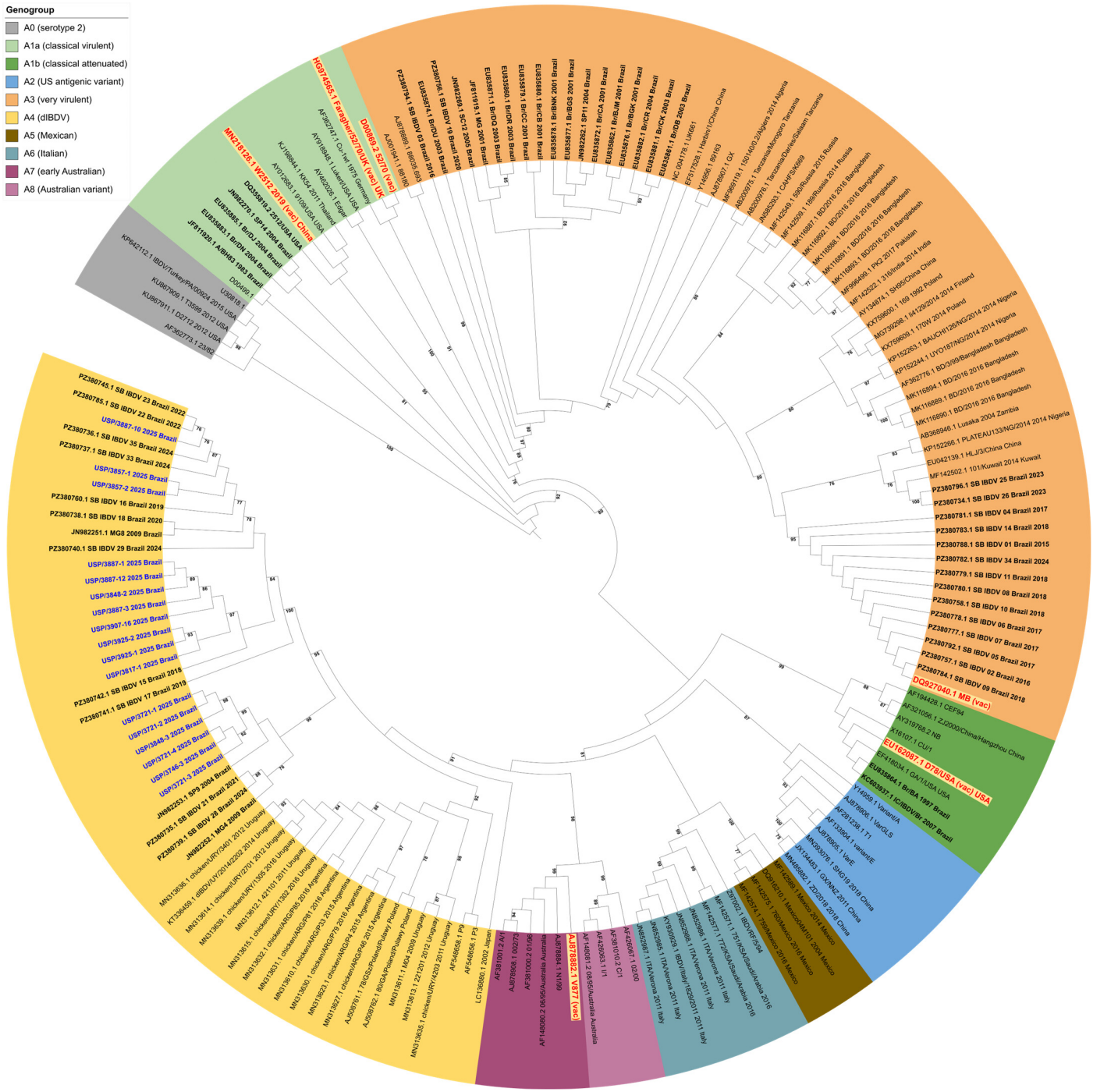


Figure 2. Maximum-likelihood phylogenetic analysis of IBDV segment A (VP2). Maximum-likelihood phylogenetic tree based on a 366-bp VP2 alignment of 176 IBDV sequences. The tree was reconstructed using the GTR+G+I model, selected by the Bayesian Information Criterion (BIC) in PhyML v3.3, with an estimated proportion of invariant sites of 0.265 and gamma shape parameter of 0.910. Genogroups were assigned according to Islam et al. (2021) [22]. Sequences generated in the present study are shown in blue, whereas previously reported Brazilian sequences are shown in bold. Vaccine reference strains are highlighted in bold red and labeled "(vac)". The tree was visualized and edited using iTOL v7.

Maximum-likelihood analysis of the VP1 dataset resolved the sequences into the previously established Segment B genogroups B1–B5, with an additional distinct cluster corresponding to the proposed novel B6 lineage (Figure 3). The B1 (classical-like) genogroup was the most broadly represented and included numerous Brazilian

sequences spanning different sampling periods, together with sequences from Argentina and Uruguay, indicating extensive circulation of segment-B classical-like viruses in South America. Brazilian sequences were also distributed among the B2 (very virulent-like) genogroup, which showed a broader geographic distribution encompassing strains from multiple countries. Within B1, the Brazilian sequences generated in the present study were interspersed among previously characterized Brazilian and South American strains rather than forming a single recent cluster, indicating that they were phylogenetically related to previously characterized Brazilian and South American B1 sequences.

In contrast, the newly identified B cluster comprised three Brazilian VP1 sequences sampled in 2020, 2023 [40], and 2025, the latter generated in the present study, and formed a distinct and well-resolved phylogenetic cluster separated from the previously established B1–B5 genogroups. We propose to name it B6. The presence of B6 across different sampling years indicates that this lineage was not restricted to a single sampling event. According to the criteria proposed by Islam et al. (2021) [22], a candidate new Segment B genogroup should comprise at least three detected strains from two different outbreaks and form a distinct cluster from previously recognized lineages. The three B6-associated VP1 sequences originated from Brazilian commercial broiler flocks sampled in 2020, 2023, and 2025. Considering the short production cycle of commercial broiler flocks (typically no longer than 50 days) and the nucleotide identities of 93.12–96.76% among these sequences, these detections are consistent with three independent outbreaks. Therefore, the proposed B6 lineage meets the minimum criteria suggested by Islam et al. (2021) [22], forming a distinct, well-supported phylogenetic cluster.

In the present study, 21 strains were sequenced, yielding 17 VP2 and 15 VP1 fragments. All 17 VP2 sequences were classified as genogroup A4, whereas 14 VP1 sequences were classified as genogroup B1 and one as B6 (Table S2). Both genomic segments were successfully obtained from 11 samples, allowing assignment of genomic constellations according to the two-segment classification scheme. Of these, 10 were classified as A4B1 and one as A4B6.

Analysis of Brazilian IBDV sequences with paired VP2 and VP1 data, including sequences generated in the present study and sequences reported in previous studies, revealed a diverse distribution of Segment A–Segment B genomic constellations (Figure 4). Among VP2 sequences, genogroups A3 ($n = 29$) and A4 ($n = 23$) predominated, whereas VP1 sequences were mainly classified as B1 ($n = 27$) or B2 ($n = 26$). The most frequent genomic associations were A3B2 and A4B1. The A3B2 constellation was detected in Brazilian sequences collected between 2001 and 2024, whereas A4B1 was identified across a broader temporal range, from 1983 to 2025. In contrast, genogroup B6 was uncommon ($n = 3$) and was associated with both A3 and A4 Segment A backgrounds. Thus, although A3B2 and A4B1 represented the predominant genomic constellations, B6 occurred in distinct Segment A backgrounds, resulting in A3B6 and A4B6 associations (Figure 4).

The combined analysis of VP2 and VP1 sequences identified two predominant genomic constellations among Brazilian IBDV sequences, A3B2 and A4B1, which were detected over comparatively broad temporal ranges (2001–2024 and 1983–2025, respectively). In contrast, the A3B6 and A4B6 constellations were represented by fewer sequences and were detected in the more recent portion of the dataset. The occurrence of B6 in both A3 and A4 Segment A backgrounds is compatible with a putative reassortment hypothesis involving B6-containing viruses and viruses carrying established A3 or A4 Segment A lineages (Figure 5). An alternative scenario involving successive reassortment events cannot be excluded. Other evolutionary scenarios, including independent reassortment events involving B6 and distinct Segment A backgrounds, also remain possible.

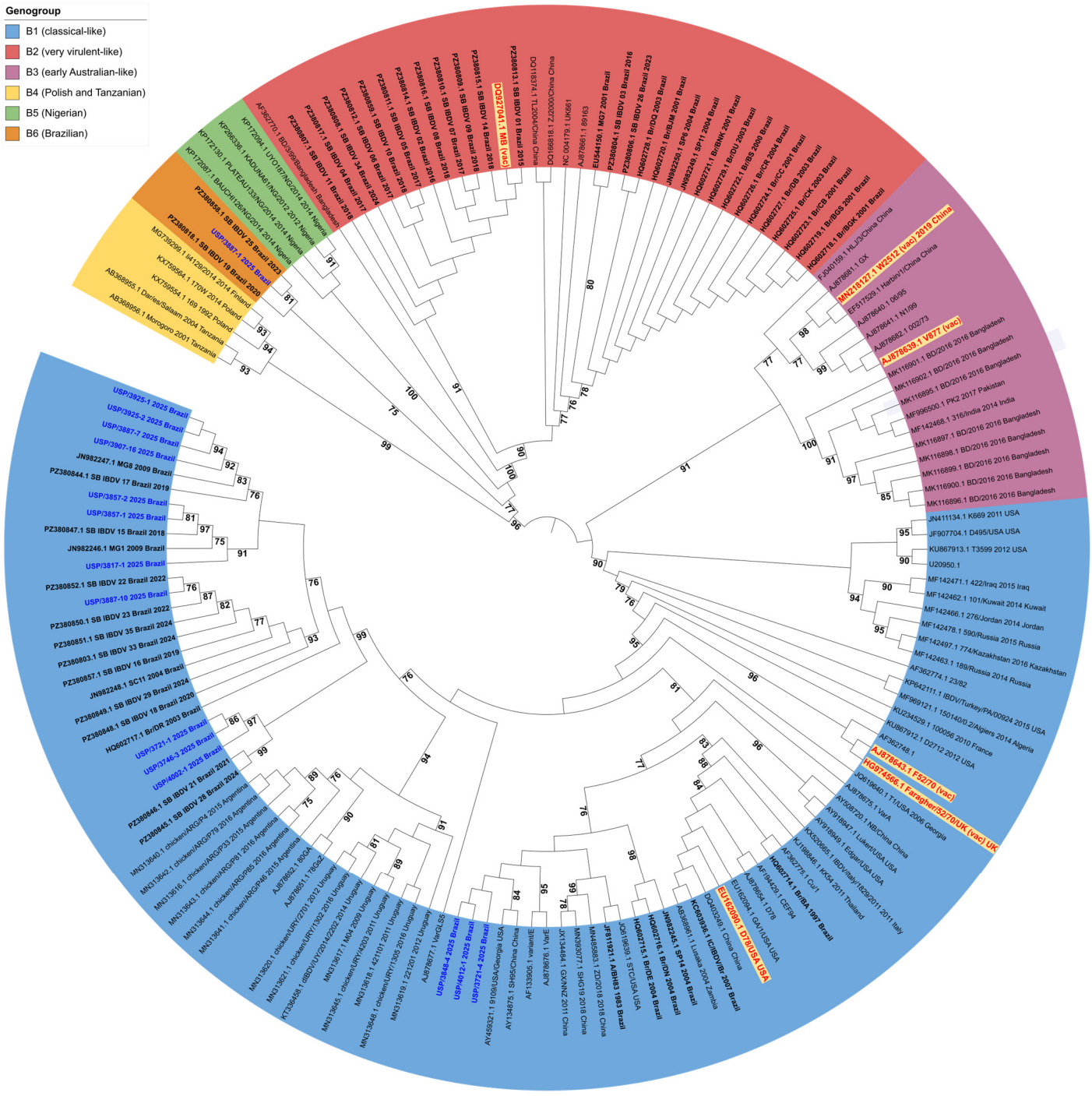


Figure 3. Maximum-likelihood phylogenetic analysis of IBDV segment B (VP1). Maximum-likelihood phylogenetic tree based on a 508-bp VP1 alignment of 157 IBDV sequences. The tree was reconstructed using the GTR+G+I model, selected by the Bayesian Information Criterion (BIC) in PhyML v3.3, with an estimated proportion of invariant sites of 0.401 and gamma shape parameter of 0.578. Genogroups were assigned according to Islam et al. (2021) [22], and the proposed B6 ("Brazilian") genogroup is indicated separately. Sequences generated in the present study are shown in blue, whereas previously reported Brazilian sequences are shown in bold. Vaccine reference strains are highlighted in bold red and labeled "(vac)". The tree was visualized and edited using iTOL v7.

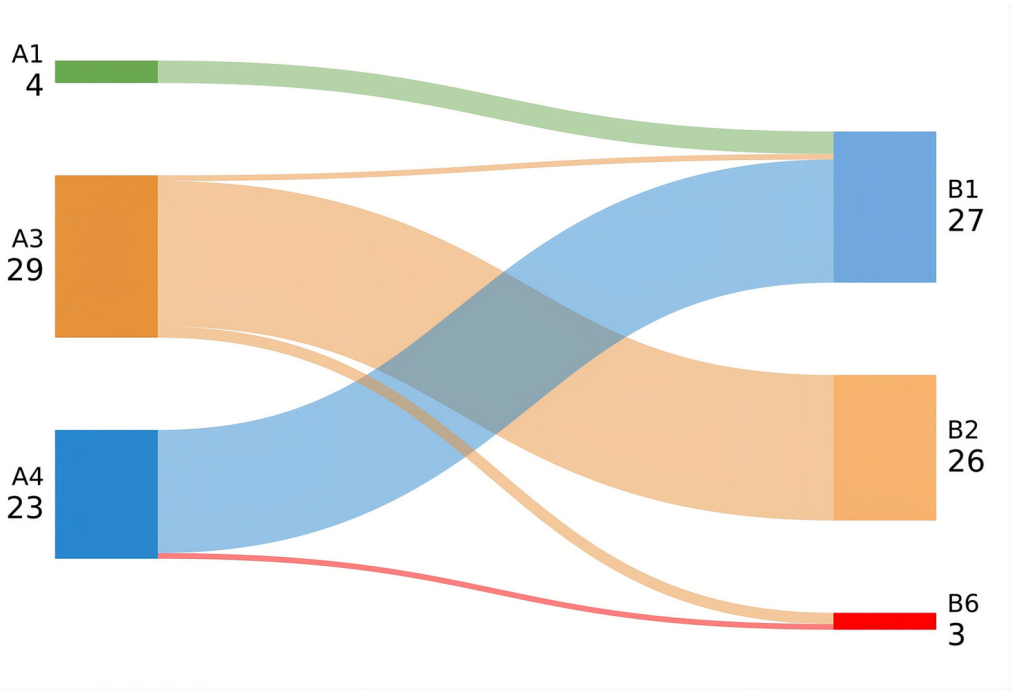


Figure 4. Sankey diagram showing the distribution of IBDV genogroup combinations between VP2 (segment A) and VP1 (segment B). The diagram illustrates the correspondence between VP2 genogroups A1, A3, and A4 and VP1 genogroups B1, B2, and B6. The width of each flow is proportional to the number of sequences assigned to each VP2–VP1 genogroup combination.

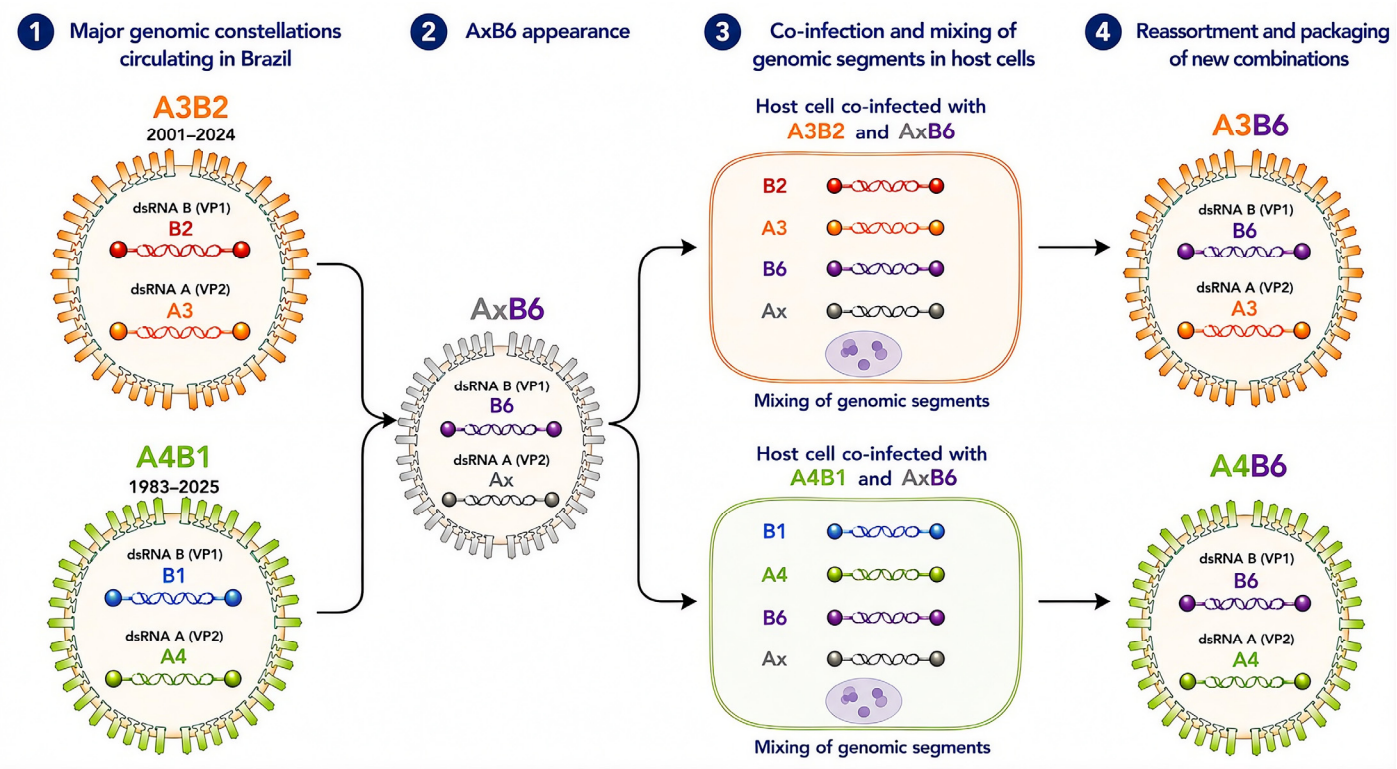


Figure 5. Hypothetical reassortment scenario in Brazilian infectious bursal disease virus (IBDV). Schematic representation of a proposed reassortment pathway involving the B6 VP1 lineage. The predominant genomic constellations identified among Brazilian IBDV sequences, A3B2 and A4B1, are shown at the initial stage, with their observed temporal ranges (2001–2024 and 1983–2025, respectively). A putative AxB6 virus, representing a B6 segment associated with an unresolved segment-A background (Ax), is shown as the potential source of the B6 lineage. Co-infection of host

cells by A3B2 and AxB6, or by A4B1 and AxB6, could allow reassortment between the two genomic segments. The resulting genomic constellations A3B6 and A4B6 are shown as potential reassortant viruses.

In the sequence identity analysis for VP2, nucleotide identities within the Brazilian-associated genogroups ranged from 92.35 to 100.00% for A1, 89.89 to 100.00% for A3, and 86.61 to 100.00% for A4 (Table S3). Comparisons with all remaining Segment A genogroups yielded broader identity ranges of 68.85–96.45% for A1, 66.12–94.81% for A3, and 67.49–94.26% for A4 (Table S4). Amino acid identities were similarly high within each lineage, ranging from 87.60 to 100.00% for A1, 90.91 to 100.00% for A3, and 86.78 to 100.00% for A4 (Table S5), whereas comparisons with the remaining genogroups ranged from 62.81 to 97.52%, 61.16 to 97.52%, and 60.33 to 93.39%, respectively (Table S6). Overall, these identity patterns were consistent with the phylogenetic clustering observed within the Brazilian-associated genogroups and indicated high sequence conservation within each genogroup.

In the sequence identity analysis for VP1, the Brazilian-associated genogroups showed high within-group conservation, with nucleotide identities ranging from 88.87–100.00% in B1, 95.93–100.00% in B2, and 93.12–96.76% in the newly identified B6 (Table S7). Comparisons with all other Segment B genogroups yielded identity ranges of 83.65–91.73% for B1, 83.65–90.49% for B2, and 86.62–91.67% for B6 (Table S8). At the amino acid level, within-group identities ranged from 76.76 to 100.00% for B1, 96.36 to 100.00% for B2, and 98.17 to 98.78% for B6 (Table S9), whereas comparisons with other genogroups ranged from 74.34 to 99.40%, 74.34 to 98.21%, and 76.19 to 97.62%, respectively (Table S10).

Amino acid alignments of Brazilian IBDV sequences revealed overall high conservation within VP2 genogroups A3 and A4, with sequence variation concentrated at specific positions, including residues located within exposed surface loops. The P_{BC} (220–224; Peak A), P_{DE} (249–254), P_{FG} (283–287), and P_{HI} (316–324; Peak B) loops were examined in both genogroups (Figures S2 and S3). The P_{BC} loop was highly conserved in A4, with the predominant sequence YQSGG, whereas A3 sequences showed a closely related YQA/PGG pattern. In the P_{DE} loop, A3 sequences were highly conserved, with the predominant QTSVQG motif, whereas A4 exhibited greater variation, including QTS/NVQ/DD/N patterns. In contrast, the P_{FG} loop was completely conserved between the two genogroups, with TAGTD as the predominant sequence in both A3 and A4. The P_{HI} loop showed a predominantly conserved KSGGQAGDQ sequence in A3, whereas A4 displayed greater variation, including KSGGQ/VA/TGDQ patterns. Overall, these comparisons indicated that amino acid variation within Brazilian VP2 sequences was not uniformly distributed, with the greatest differences between A3 and A4 observed in the P_{BC}, P_{DE}, and P_{HI} exposed loops, whereas P_{FG} remained highly conserved.

Amino acid alignments of Brazilian IBDV VP1 sequences revealed an even higher degree of conservation than that observed for VP2, particularly within genogroup B1 (Figures S4 and S5). B1 sequences were highly conserved, with only a few notable polymorphisms, including V160I and D219N in some Brazilian sequences, D219E in European and Asian sequences, and F243P in Uruguayan and Argentinian sequences. Genogroup B2 showed comparatively greater amino acid variation, including T96N in Brazilian sequences; E146D and G147N, predominantly among Brazilian sequences; D161A and D242E, also frequent among Brazilian sequences; A163V in some Brazilian sequences; and D219E and D219N in a subset of Brazilian sequences. The B6 amino acid profile also differed from the other Segment B genogroups, with notable differences from B4 at positions 141, 145, 147, and 163 (Figure S6). Overall, these alignments indicated greater amino acid conservation in VP1 than in VP2, with B1 displaying the highest degree of conservation among the analyzed genogroups. Pairwise amino acid identity between

the 51 Brazilian A4 VP2 sequences and the vaccine reference strains ranged from 85.12–92.56% for Faragher 52/70, 85.12–93.39% for Winterfield 2512, 85.12–92.56% for D78, 83.47–90.08% for V877, and 84.30–91.74% for MB (Table S5). Multiple amino acid differences were observed within the VP2 hypervariable region, including positions 241, 245, 258, 264, 276, 280, 289–291, 296, 299, 300, 305, and 309, with variation also evident within the PDE and PHI loops (Figure S7).

Estimates of mean evolutionary distances further supported the genetic differentiation observed among the Segment A genogroups (Table 4). The A0 (serotype 2) genogroup showed the highest mean evolutionary distances relative to the other Segment A genogroups, ranging from 0.604 to 0.713 substitutions per site. Among the Brazilian-associated genogroups, A1, A3, and A4 showed mean distances of 0.085–0.169, 0.090–0.198, and 0.129–0.206 substitutions per site, respectively, when compared with the other A1–A8 genogroups.

Table 4. Estimates of evolutionary distances between IBDV segment A genogroups based on the partial VP2 nucleotide sequences analyzed in this study. *.

Genogroup	A0	A1	A2	A3	A4	A5	A6	A7	A8
A0 (serotype 2)	–			–					
A1 (classical)	0.604	–							
A2 (US antigenic variant)	0.684	0.085	–						
A3 (very virulent)	0.659	0.090	0.121	–					
A4 (dIBDV)	0.644	0.129	0.150	0.162	–				
A5 (Mexican)	0.713	0.124	0.132	0.171	0.167	–			
A6 (Italian)	0.620	0.114	0.140	0.174	0.181	0.176	–		
A7 (early Australian)	0.692	0.169	0.194	0.197	0.206	0.235	0.205	–	
A8 (Australian variant)	0.639	0.163	0.185	0.198	0.199	0.209	0.203	0.162	–

* Values represent the mean number of nucleotide substitutions per site across all intergenogroup sequence pairs. Evolutionary distances were estimated using the Maximum Composite Likelihood model [35], incorporating gamma-distributed rate variation (shape parameter = 1). The analysis included 176 nucleotide sequences. Ambiguous sites were treated by pairwise deletion, yielding 366 positions in the final alignment. Analyses were performed in MEGA12 [36].

For Segment B (Table 5), B1, B3, and B6 showed mean evolutionary distances of 0.127–0.165, 0.131–0.182, and 0.112–0.131 substitutions per site, respectively, relative to the other Segment B genogroups. Notably, B6 exceeded the 12% nucleotide-divergence threshold proposed by Islam et al. (2021) [22] when compared with four of the five previously recognized Segment B genogroups, while showing a closely comparable divergence of 11.2% relative to B4. Together with the well-resolved phylogenetic clustering of B6, its representation by three Brazilian sequences from different sampling years, and its distinct position relative to the established B1–B5 lineages, these evolutionary-distance estimates provide additional evidence supporting B6 as a distinct Segment B genogroup.

Table 5. Estimates of evolutionary distances between IBDV segment B genogroups based on the partial VP1 nucleotide sequences analyzed in this study. *.

Genogroup	B1	B2	B3	B4	B5	B6
B1 (classical-like)	–					
B2 (very virulent-like)	0.165	–				
B3 (early Australian-like)	0.139	0.178	–			
B4 (Polish and Tanzanian)	0.145	0.154	0.157	–		
B5 (Nigerian)	0.127	0.184	0.182	0.172	–	

B6 (Brazilian)	0.127	0.130	0.131	0.112	0.131	–

* Values represent the mean number of nucleotide substitutions per site across all intergenogroup sequence pairs. Evolutionary distances were estimated using the Maximum Composite Likelihood model [36], incorporating gamma-distributed rate variation (shape parameter = 1). The analysis included 157 nucleotide sequences. Ambiguous sites were treated by pairwise deletion, yielding 508 positions in the final alignment. Analyses were performed in MEGA12 [36].

3.3. Selective Pressure and Recombination Analyses

Selection analyses of VP2 revealed a predominance of purifying selection in both A3 and A4. FEL identified 51 codons under purifying selection in A3 (Table S13, Figure S8) and 54 in A4 (Table S14, Figure S9), whereas no codons in A3 showed evidence of pervasive positive selection. In A4, a single codon (253) was identified under pervasive positive selection (p = 0.067) (Figure S10). MEME detected four sites under episodic diversifying selection in each genogroup, corresponding to codons 222 (p = 0.009), 328 (p = 0.06), 330 (p = 0.009), and 334 (p = 0.023) in A3 (Table S11), and 253 (p = 0.058), 317 (p = 0.004), 320 (p = 0.005), and 324 (p = 0.014) in A4 (Table S12). In A3, codon 222 mapped to the P_{BC} loop (219–224; Peak A), whereas codons 328, 330, and 334 were located downstream of the P_{HI} loop (316–324; Peak B) (Figure 6A). In contrast, in A4, codon 253 mapped to the P_{DE} loop (249–254), whereas codons 317, 320, and 324 mapped directly within the P_{HI} loop (Figure 6B). Notably, codon 253 in A4 was identified by both FEL and MEME, whereas none of the MEME-positive sites in A3 showed evidence of pervasive positive selection by FEL. Overall, episodic diversification involved exposed regions of VP2 in both genogroups, but was more directly concentrated within the characterized surface loops in A4.

Exploratory recombination analysis using RDP5 did not identify putative recombination events supported by at least five independent detection methods in any of the VP1 or VP2 fragments analyzed. These findings should nevertheless be interpreted cautiously, given the relatively short sequence fragments analyzed, which may reduce the ability of recombination-detection methods to identify events and accurately localize recombination breakpoints.

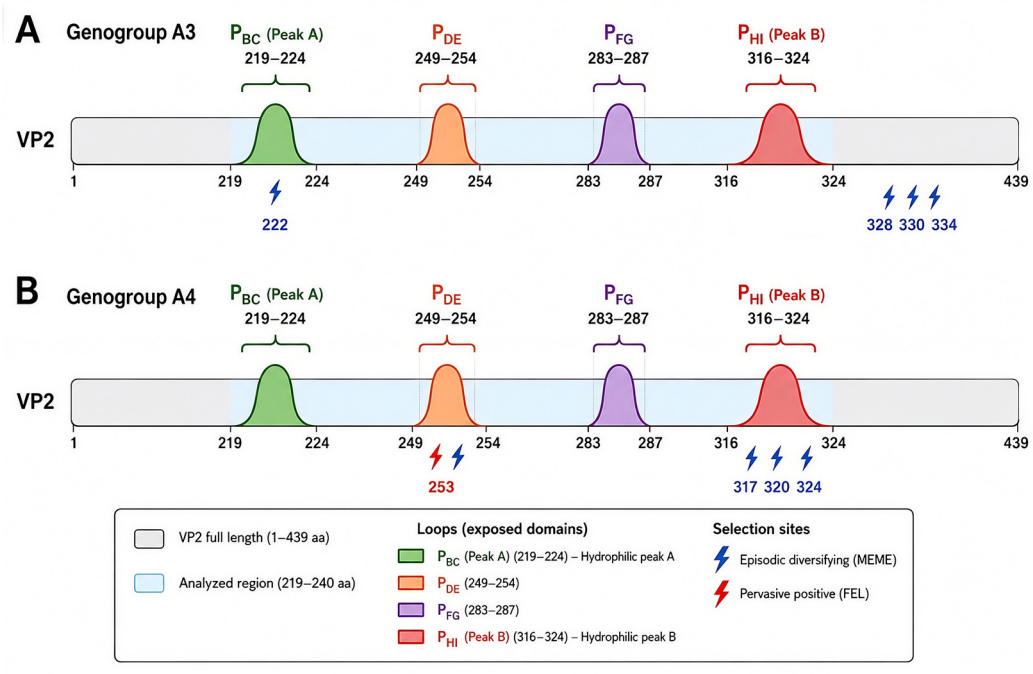


Figure 6. Distribution of positively selected sites in VP2 of IBDV genogroups A3 and A4. The VP2 protein (1–439 aa) is shown with the analyzed region highlighted in light blue and the exposed loops

P_{BC} (219–224; Peak A), P_{DE} (249–254), P_{FG} (283–287), and P_{HI} (316–324; Peak B). Blue lightning bolts indicate episodically diversifying sites detected by MEME ($p < 0.1$), whereas red lightning bolts indicate pervasive positive selection detected by FEL ($p < 0.1$). (**A**) A3: MEME sites 222, 328, 330, and 334; no sites were detected by FEL. (**B**) A4: MEME sites 253, 317, 320, and 324; FEL identified site 253. MEME sites retaining significance at $p < 0.05$ were codons 222, 330, and 334 in A3 and codons 317, 320, and 324 in A4.

4. Discussion

The high detection rate of IBDV in underperforming Brazilian commercial flocks highlights the continued importance of this pathogen under contemporary field conditions. Beyond its persistent circulation, however, the current epidemiological landscape may reflect a dynamic interplay between established viral lineages, geographic and temporal persistence, host and production factors, and ongoing genomic diversification. Understanding how these processes shape the circulation and evolution of IBDV is particularly relevant in a country with an extensive and highly productive poultry industry, where viral adaptation may have important consequences for disease control and vaccination strategies.

The high IBDV detection rate observed in the present study (85.4%) indicates that IBDV remains frequently detectable among Brazilian commercial flocks submitted for investigation of clinical or production-related problems. However, this estimate should be interpreted in the context of the sampling strategy, as samples were obtained from flocks with suspected IBDV infection and/or clinical signs compatible with immunosuppression and therefore do not represent a population-based prevalence estimate. Field viruses were predominantly detected after the second week of age, particularly during the 15–42-day period, although infections before 14 days were also observed. This age distribution is consistent with the recognized epidemiology of IBDV, as susceptibility to infection increases as maternally derived antibodies decline [1,41,42]. Early infection (<14 days of age) is particularly concerning because the bursa of Fabricius is still undergoing maturation, and viral replication can cause extensive damage to immature B lymphocytes, potentially resulting in severe and persistent immunosuppression and contributing to reduced productivity and increased sanitary disturbances. Infections after second week of age can also cause immunosuppression and the severity will depend on the pathogenicity of the virus involved [2,43]. High viral pressure may further favor infection at very young ages, particularly in farms with repeated litter reuse [44,45].

The age-related pattern also differed according to production type, with IBDV-positive samples virus detection occurring earlier in broilers than in layer flocks. This observation is consistent with field monitoring of the bursa of Fabricius, which has indicated earlier infection in broilers than in layers. The delayed onset of infection in layers may be related to their higher and more persistent levels of maternally derived antibodies, resulting in a longer period of passive protection [46,47]. Taken together, the frequent detection of IBDV across multiple Brazilian states and the predominance of infection after the second week of life, together with occasional very early infections, highlight the continued epidemiological importance of IBDV and provide an important context for interpreting the genomic diversity identified in the present study.

The identification of A4 in all 17 VP2 sequences generated in the present study, together with the presence of historical Brazilian sequences within the same genogroup, supports the continued circulation of the A4 Segment-A lineage in Brazil. A4, corresponding to the former distinct IBDV (dIBDV) genogroup, has been predominantly associated with South American IBDV populations and has been repeatedly detected in Brazil, where related antigenic-variant viruses have been documented over several

decades [13,24,26,27,40]. In the present phylogeny, Brazilian A4 sequences showed a more pronounced geographic structure than A3 sequences, with Brazilian sequences forming closely related clusters that were distinguishable from sequences from neighboring countries. This pattern may reflect prolonged local circulation and diversification of A4 within Brazilian poultry populations rather than repeated independent introductions. Importantly, the broad temporal representation of A4, extending from historical sequences to the viruses characterized in the present study, together with its repeated detection in Brazil, supports its interpretation as an established endemic lineage rather than a sporadically introduced virus. Its continued detection in contemporary samples is particularly relevant because A4-associated infections may be less conspicuous clinically than infections caused by highly virulent A3 viruses, potentially resulting in underrepresentation in outbreak-oriented surveillance and sequencing efforts. The persistence of A4 across historical and contemporary samples nevertheless demonstrates that this lineage remains genetically relevant in Brazil.

The VP1 analysis revealed that B1 and B2 remain the principal segment-B genogroups associated with Brazilian IBDV sequences, consistent with the broad distribution of classical-like and very virulent-like segment-B lineages (respectively) reported in South American populations [40]. More notably, three Brazilian sequences collected in 2020, 2023, and 2025 formed a distinct and well-resolved cluster separated from the previously established B1–B5 genogroups. The combination of phylogenetic separation, temporal persistence, and substantial nucleotide divergence supports the recognition of B6 as a distinct segment-B genogroup. Also, the distinct B6 amino acid profile, with variation across positions 141–163, provides additional molecular support for its differentiation from previously recognized Segment B genogroups. Thus, B6 should be regarded as a novel segment-B genogroup within the present classification framework, rather than merely as a divergent Brazilian sequence cluster. These findings identify a previously unrecognized Brazilian segment-B lineage whose distribution and evolutionary stability warrant further investigation. The detection of B6 in samples separated by several years also argues against its interpretation as a single recent sequencing or outbreak-associated anomaly and raises the possibility of a more prolonged circulation that has remained largely undetected because molecular surveillance in Brazil has historically focused on VP2.

Analysis of paired VP2–VP1 sequences revealed two major genomic constellations, A3B2 and A4B1, which were detected across substantially different but extended temporal ranges. A3B2 was represented by Brazilian sequences collected from 2001 to 2024, potentially reflecting repeated introductions, whereas A4B1 extended from 1983 to 2025, consistent with a highly established and geographically distributed lineage. In accordance with previous reports, A3B2 is predominantly associated with very virulent IBDV strains and acute clinical disease, whereas A4B1 has been associated with distinct, often subclinical field infections characterized by bursal atrophy and inflammation [22,48–50]. The substantially broader temporal representation of A4B1, including sequences from the present study, further supports the epidemiological importance of A4-associated viruses in Brazil. Conversely, the conspicuous clinical manifestations associated with very virulent A3 viruses may increase their likelihood of being detected during diagnostic investigations and subsequently selected for molecular characterization, potentially contributing to an apparent prominence of A3 in surveillance datasets that does not necessarily reflect its relative prevalence in the field. The persistence of these constellations over decades is consistent with the establishment and continued circulation of various segment-A/segment-B genomic backgrounds within Brazilian poultry populations. Their contrasting temporal and phylogenetic patterns further reinforce the importance of considering both genomic segments when describing IBDV diversity,

because classification based solely on VP2 would obscure the Segment-B component and potentially mask reassortant viruses or reassortment events. In addition, both segments contribute to the pathogenicity of IBDV strains. Genome reassortment has been documented among IBDV strains belonging to different pathotypes [17,18,51]. The broad temporal representation of A3B2 and A4B1 provides an important baseline against which the more recently detected A3B6 and A4B6 combinations can be interpreted. Nevertheless, temporal overlap among lineages and incomplete historical sampling prevent direct inference of the chronological emergence of individual genomic constellations.

A particularly notable finding was the association of the B6 segment with two distinct segment-A backgrounds, A3 and A4, resulting in A3B6 and A4B6 genomic constellations. Because IBDV possesses a bisegmented genome, co-infection of a host cell by viruses carrying distinct segment-A and segment-B combinations provides a mechanistic basis for reassortment and the generation of novel genomic constellations [52,53]. The presence of B6 in both A3 and A4 backgrounds is therefore compatible with a putative reassortment scenario involving a B6-containing virus and viruses carrying established A3 or A4 segment-A lineages. The temporal distribution further permits a plausible scenario in which a B6-containing virus circulated before the emergence or detection of the more recent A3B6 and A4B6 combinations. However, the available data do not establish the direction, timing, or number of reassortment events. In particular, A3B6 could have arisen independently from A4B6, or a sequential process could have involved an initial A3B6 virus followed by reassortment with an A4B1 virus. Consequently, the present evidence should be interpreted as supporting a putative reassortment hypothesis, rather than demonstrating a specific historical reassortment pathway. Analyses of reassortant viruses have shown that segment A determines the virulence but segment B also influences the pathogenicity [15,17,18]. Thus, future investigations analyzing segments A and B of the virus should be conducted to determine the spread of the B6-associated virus, given the potential implications in terms of pathogenicity.

The amino acid analysis demonstrated that VP2 variation was not uniformly distributed across the protein and was particularly evident within several exposed surface loops. The P_{BC}, P_{DE}, and P_{HI} regions showed differential amino acid patterns between A3 and A4, whereas the P_{FG} loop displayed the conserved TAGTD motif in both genogroups. These observations are relevant because the exposed loops of the VP2 hypervariable region contribute to the structural and antigenic properties of the viral capsid and contain residues involved in interactions with host–cell receptors and neutralizing antibodies [7,54,55]. The greater sequence heterogeneity observed in specific loops of A4 compared with the conserved P_{FG} region suggests that evolutionary constraints may differ substantially even among adjacent exposed regions. Consistent with this pattern, comparison with vaccine reference strains revealed 83.47–93.39% amino acid identity between Brazilian A4 sequences and the five vaccine strains examined, with differences also occurring at several positions within the hypervariable region, particularly in the PDE and PHI loops. None of the vaccine reference strains analyzed belonged to A4, whereas the MB reference was assigned to A3. However, sequence variation alone cannot establish altered antigenicity, receptor usage, or vaccine escape. Functional studies, including antigenic characterization and experimental assessment of representative variants, would be required to determine whether the observed substitutions have phenotypic consequences. Thus, the present findings primarily establish a molecular pattern of localized variation within regions of known structural and antigenic relevance.

The selection analyses provided additional evidence that evolutionary constraints are heterogeneous across VP2. The predominance of purifying selection in both A3 and A4 is consistent with strong functional constraints acting on the capsid protein, while the detection of episodic diversifying selection at a limited number of sites indicates that

particular residues may experience lineage-specific or transient selective pressures [56,57]. Notably, A3 showed an episodically diversifying site within the P_{BC} loop and additional sites immediately downstream of the P_{HI} loop, whereas A4 displayed episodically diversifying sites directly within the P_{DE} and P_{HI} loops. In A4, codon 253 within P_{DE} was identified by both FEL and MEME, providing stronger evidence for selection at this position than for the MEME-only sites. The concentration of selected sites around exposed regions of VP2 is compatible with the possibility that host immune pressure contributes to localized diversification, although other selective forces, including receptor interactions or functional constraints associated with capsid structure, cannot be excluded [56,58]. Importantly, the absence of pervasive positive selection at the corresponding A3 sites indicates that the evolutionary dynamics of these exposed regions may differ between genogroups rather than reflecting a uniform selective process across VP2. These site-level analyses were exploratory, and sites detected only at $p < 0.1$ should be interpreted cautiously.

No recombination events in the analyzed VP1 or VP2 fragments met the predefined criterion of support by at least five independent detection methods. This finding provides no evidence for detectable homologous recombination within the analyzed regions, although the relatively short sequence fragments substantially limit the ability of recombination-detection methods to identify events or accurately localize breakpoints [59]. In this context, the discordant association of B6 with A3 and A4 is more directly compatible with reassortment between the two genomic segments than with intrasegment recombination. Nevertheless, the distinction cannot be resolved completely from partial sequences alone, and the proposed evolutionary scenarios remain provisional. Continued surveillance of B6-associated viruses, particularly A4B6, together with broader temporal and geographic sampling and generation of longer or complete VP1 and VP2 sequences, will be essential to determine whether this constellation represents a sporadic reassortment product or a lineage capable of sustained circulation. Expanded genomic surveillance would also help clarify the origin and evolutionary history of B6 and determine whether additional reassortant constellations remain undetected in Brazilian poultry populations.

5. Conclusions

This study provides an integrated characterization of IBDV circulating in Brazilian commercial poultry based on the analysis of both genomic segments. The results demonstrate substantial genomic diversity, with A4 emerging as the predominant Segment-A lineage among newly generated VP2 sequences and showing evidence of prolonged and continued circulation in Brazil, while A3B2 and A4B1 represented the major bisegment genomic constellations identified in the broader Brazilian dataset. The identification of B6 as a novel Segment-B genogroup and its association with both A3 and A4 Segment-A backgrounds resulted in the detection of A3B6 and A4B6 constellations, providing molecular evidence compatible with reassortment and highlighting previously unrecognized segment-level diversity in Brazilian IBDV populations. In addition, localized amino acid variation and episodic diversification were identified within exposed regions of VP2, particularly among the P_{BC}, P_{DE}, and P_{HI} loops, whereas no supported intrasegment recombination was detected. These findings emphasize the value of incorporating both genomic segments into IBDV surveillance and suggest that current control strategies, including vaccination programs, should be continuously reassessed in light of the genetic and epidemiological diversity of viruses circulating in Brazil. Continued genomic surveillance, including paired or complete VP1 and VP2 sequencing across broader temporal and geographic sampling, will be essential to clarify the evolutionary history of B6, determine the persistence of the newly identified genomic

constellations, and anticipate their potential implications for IBDV pathogenicity and control in Brazil.

Supplementary Materials: The following supporting information can be downloaded at https://www.mdpi.com/article/10.3390/pathogens15111152/s1, Figure S1: Geographic distribution of IBDV detection in Brazil; Figure S2: Amino acid polymorphisms in IBDV A3 VP2 sequences; Figure S3: Amino acid polymorphisms in IBDV A4 VP2 sequences; Figure S4: Amino acid polymorphisms in IBDV B1 VP1 sequences; Figure S5: Amino acid polymorphisms in IBDV B2 VP1 sequences; Figure S6: Amino acid polymorphisms in IBDV B6 VP1 sequences compared with other genogroups; Figure S7: VP2 amino acid variation in Brazilian IBDV A4 sequences compared with vaccine reference strains and representative sequences from other genogroups; Figure S8: FEL analysis of IBDV A3 VP2 sequences; Figure S9: FEL analysis of IBDV A4 VP2 sequences; Figure S10: Phylogenetic distribution of pervasive positive selection at codon 253 in IBDV A4 VP2 sequences; Table S1: Clinical and epidemiological characteristics of IBDV-positive and -negative samples; Table S2: IBDV genogroup and bisegmented genotype assignments of sequenced samples; Table S3: Pairwise nucleotide sequence identity among IBDV VP2 sequences; Table S4: VP2 nucleotide sequence identity ranges (%) among IBDV genogroups; Table S5: Pairwise amino acid sequence identity among IBDV VP2 sequences; Table S6: VP2 amino acid sequence identity ranges (%) among IBDV genogroups; Table S7: Pairwise nucleotide sequence identity among IBDV VP1 sequences; Table S8: VP1 nucleotide sequence identity ranges (%) among IBDV genogroups; Table S9: Pairwise amino acid sequence identity among IBDV VP1 sequences; Table S10: VP1 amino acid sequence identity ranges (%) among IBDV genogroups; Table S11: Episodic diversifying selection detected in IBDV A3 VP2 sequences using MEME; Table S12: Episodic diversifying selection detected in IBDV A4 VP2 sequences using MEME. Table S13: Pervasive selection detected in IBDV A3 VP2 sequences using FEL; Table S14: Pervasive selection detected in IBDV A4 VP2 sequences using FEL.

Author Contributions: Conceptualization, J.L.C., R.D.C. and A.J.P.F.; methodology, J.L.C., C.N. and B.F.; formal analysis, J.L.C. and R.D.C.; investigation, J.L.C., C.N., B.F., B.A., R.D.C. and A.J.P.F.; writing—original draft preparation, J.L.C. and R.D.C.; writing—review and editing, J.L.C., C.N., B.F., B.A., R.D.C. and A.J.P.F.; supervision, A.J.P.F.; funding acquisition, A.J.P.F. All authors have read and agreed to the published version of the manuscript.

Funding: This research was partly funded by the Conselho Nacional de Pesquisa e Desenvolvimento Tecnológico (CNPq), grant number 301084/2019-0.

Institutional Review Board Statement: The requirements for ethical review and approval were waived for this study because of the National Council for the Control of Animal Experimentation (CONCEA) Resolution, Chapter III "Procedures: Article 8 Research, teaching, or extension protocols that do not use live animals or that use only biological samples of animal origin or cadavers, without the handling of live vertebrate animals by the researchers involved, are exempt from submission to the National Council for the Control of Animal Experimentation (CONCEA)", Item 6.1.10 of ANNEX 1 of Normative Resolution No. 55, of 5 October 2022.

Informed Consent Statement: Not applicable.

Data Availability Statement: The assembled sequences were deposited in GenBank under accession numbers QB006137 to QB006151 (VP1 sequences) and QB006191 to QB006207 (VP2 sequences.

Acknowledgments: The authors would like to thank Christophe Cazaban for his valuable review and constructive comments on the manuscript.

Conflicts of Interest: The authors declare no conflicts of interest.

References

1. Eterradossi, N.; Saif, Y.M. Infectious Bursal Disease. In *Diseases of Poultry*, 14th ed.; Swayne, D.E., Boulianne, M., Logue, C.M., McDougald, L.R., Nair, V., Suarez, D.L., de Witt, S., Grimes, T., Johnson, D., Kromm, M., et al., Eds.; John Wiley & Sons Ltd.: Hoboken, NJ, USA, 2020; Volume 1, pp. 257–283.
2. Sharma, J.M.; Kim, I.J.; Rautenschlein, S.; Yeh, H.Y. Infectious Bursal Disease Virus of Chickens: Pathogenesis and Immunosuppression. *Dev. Comp. Immunol.* **2000**, *24*, 223–235. https://doi.org/10.1016/s0145-305x(99)00074-9.
3. Dey, S.; Pathak, D.C.; Ramamurthy, N.; Maity, H.K.; Chellappa, M.M. Infectious Bursal Disease Virus in Chickens: Prevalence, Impact, and Management Strategies. *Vet. Med.* **2019**, *10*, 85–97. https://doi.org/10.2147/VMRR.S185159.
4. Mundt, E.; Müller, H. Complete Nucleotide Sequences of 5′- and 3′-Noncoding Regions of Both Genome Segments of Different Strains of Infectious Bursal Disease Virus. *Virology* **1995**, *209*, 10–18. https://doi.org/10.1006/viro.1995.1226.
5. Brandt, M.; Yao, K.; Liu, M.; Heckert, R.A.; Vakharia, V.N. Molecular Determinants of Virulence, Cell Tropism, and Pathogenic Phenotype of Infectious Bursal Disease Virus. *J. Virol.* **2001**, *75*, 11974–11982. https://doi.org/10.1128/JVI.75.24.11974-11982.2001.
6. Delmas, B.; Attoui, H.; Ghosh, S.; Malik, Y.S.; Mundt, E.; Vakharia, V.N.; Ictv Report Consortium. ICTV Virus Taxonomy Profile: Birnaviridae. *J. Gen. Virol.* **2019**, *100*, 5–6. https://doi.org/10.1099/jgv.0.001185.
7. Letzel, T.; Coulibaly, F.; Rey, F.A.; Delmas, B.; Jagt, E.; van Loon, A.A.M.W.; Mundt, E. Molecular and Structural Bases for the Antigenicity of VP2 of Infectious Bursal Disease Virus. *J. Virol.* **2007**, *81*, 12827–12835. https://doi.org/10.1128/JVI.01501-07.
8. Boot, H.J.; Hoekman, A.J.W.; Gielkens, A.L.J. The Enhanced Virulence of Very Virulent Infectious Bursal Disease Virus Is Partly Determined by Its B-Segment. *Arch. Virol.* **2005**, *150*, 137–144. https://doi.org/10.1007/s00705-004-0405-9.
9. Escaffre, O.; Le Nouën, C.; Amelot, M.; Ambroggio, X.; Ogden, K.M.; Guionie, O.; Toquin, D.; Müller, H.; Islam, M.R.; Eterradossi, N. Both Genome Segments Contribute to the Pathogenicity of Very Virulent Infectious Bursal Disease Virus. *J. Virol.* **2013**, *87*, 2767–2780. https://doi.org/10.1128/JVI.02360-12.
10. Gao, H.-L.; Wang, X.-M.; Gao, Y.-L.; Fu, C.-Y. Direct Evidence of Reassortment and Mutant Spectrum Analysis of a Very Virulent Infectious Bursal Disease Virus. *Avian Dis.* **2007**, *51*, 893–899. https://doi.org/10.1637/7626-042706R1.1.
11. He, C.-Q.; Ma, L.-Y.; Wang, D.; Li, G.-R.; Ding, N.-Z. Homologous Recombination Is Apparent in Infectious Bursal Disease Virus. *Virology* **2009**, *384*, 51–58. https://doi.org/10.1016/j.virol.2008.11.009.
12. Jackwood, D.J. Molecular Epidemiologic Evidence of Homologous Recombination in Infectious Bursal Disease Viruses. *Avian Dis.* **2012**, *56*, 574–577. https://doi.org/10.1637/10053-010912-ResNote.1.
13. Silva, F.M.F.; Vidigal, P.M.P.; Myrrha, L.W.; Fietto, J.L.R.; Silva, A.; Almeida, M.R. Tracking the Molecular Epidemiology of Brazilian Infectious Bursal Disease Virus (IBDV) Isolates. *Infect. Genet. Evol.* **2013**, *13*, 18–26. https://doi.org/10.1016/j.meegid.2012.09.005.
14. Patel, A.K.; Pandey, V.C.; Pal, J.K. Evidence of Genetic Drift and Reassortment in Infectious Bursal Disease Virus and Emergence of Outbreaks in Poultry Farms in India. *Virusdisease* **2016**, *27*, 161–169. https://doi.org/10.1007/s13337-016-0306-z.
15. Wei, Y.; Li, J.; Zheng, J.; Xu, H.; Li, L.; Yu, L. Genetic reassortment of infectious bursal disease virus in nature. *Biochem. Biophys. Res. Commun.* **2006**, *350*, 277–287. https://doi.org/10.1016/j.bbrc.2006.09.040.
16. Lee, H.-J.; Jang, I.; Shin, S.-H.; Lee, H.-S.; Choi, K.-S. Genome Sequence of a Novel Reassortant and Very Virulent Strain of Infectious Bursal Disease Virus. *Genome Announc.* **2017**, *5*, e00730-17. https://doi.org/10.1128/genomeA.00730-17.
17. Abed, M.; Soubies, S.; Courtillon, C.; Briand, F.-X.; Allée, C.; Amelot, M.; De Boisseson, C.; Lucas, P.; Blanchard, Y.; Belahouel, A.; et al. Infectious Bursal Disease Virus in Algeria: Detection of Highly Pathogenic Reassortant Viruses. *Infect. Genet. Evol.* **2018**, *60*, 48–57. https://doi.org/10.1016/j.meegid.2018.01.029.
18. Mató, T.; Tatár-Kis, T.; Felföldi, B.; Jansson, D.S.; Homonnay, Z.; Bányai, K.; Palya, V. Occurrence and Spread of a Reassortant Very Virulent Genotype of Infectious Bursal Disease Virus with Altered VP2 Amino Acid Profile and Pathogenicity in Some European Countries. *Vet. Microbiol.* **2020**, *245*, 108663. https://doi.org/10.1016/j.vetmic.2020.108663.
19. Müller, H.; Islam, M.R.; Raue, R. Research on Infectious Bursal Disease—The Past, the Present and the Future. *Vet. Microbiol.* **2003**, *97*, 153–165. https://doi.org/10.1016/j.vetmic.2003.08.005.
20. Hernández, M.; Tomás, G.; Marandino, A.; Iraola, G.; Maya, L.; Mattion, N.; Hernández, D.; Villegas, P.; Banda, A.; Panzera, Y.; et al. Genetic Characterization of South American Infectious Bursal Disease Virus Reveals the Existence of a Distinct Worldwide-Spread Genetic Lineage. *Avian Pathol.* **2015**, *44*, 212–221. https://doi.org/10.1080/03079457.2015.1025696.
21. Jackwood, D.J.; Schat, K.A.; Michel, L.O.; de Wit, S. A Proposed Nomenclature for Infectious Bursal Disease Virus Isolates. *Avian Pathol.* **2018**, *47*, 576–584. https://doi.org/10.1080/03079457.2018.1506092.

22. Islam, M.R.; Nooruzzaman, M.; Rahman, T.; Mumu, T.T.; Rahman, M.M.; Chowdhury, E.H.; Eterradossi, N.; Müller, H. A Unified Genotypic Classification of Infectious Bursal Disease Virus Based on Both Genome Segments. *Avian Pathol.* **2021**, *50*, 190–206. https://doi.org/10.1080/03079457.2021.1873245.
23. Wang, Y.; Fan, L.; Jiang, N.; Gao, L.; Li, K.; Gao, Y.; Liu, C.; Cui, H.; Pan, Q.; Zhang, Y.; et al. An Improved Scheme for Infectious Bursal Disease Virus Genotype Classification Based on Both Genome-Segments A and B. *J. Integr. Agric.* **2021**, *20*, 1372–1381. https://doi.org/10.1016/S2095-3119(20)63424-4.
24. Ikuta, N.; El-Attrache, J.; Villegas, P.; García, E.M.; Lunge, V.R.; Fonseca, A.S.; Oliveira, C.; Marques, E.K. Molecular Characterization of Brazilian Infectious Bursal Disease Viruses. *Avian Dis.* **2001**, *45*, 297–306.
25. Fernandes, M.J.B.; Simoni, I.C.; Harakava, R.; Rivas, E.B.; Arns, C.W. Partial VP1 Sequencing of Brazilian Infectious Bursal Disease Virus Strains. *Braz. J. Microbiol.* **2012**, *43*, 1015–1021. https://doi.org/10.1590/S1517-83822012000300024
26. Muniz, E.C.; Verdi, R.; Jackwood, D.J.; Kuchpel, D.; Resende, M.S.; Mattos, J.C.Q.; Cookson, K. Molecular Epidemiologic Survey of Infectious Bursal Disease Viruses in Broiler Farms Raised under Different Vaccination Programs. *J. Appl. Poult. Res.* **2018**, *27*, 253–261. https://doi.org/10.3382/japr/pfx043.
27. de Fraga, A.P.; Gräf, T.; Coltro, V.P.; Ikuta, N.; Fonseca, A.S.K.; Majó, N.; Lunge, V.R. Phylodynamic Analyses of Brazilian Antigenic Variants of Infectious Bursal Disease Virus. *Infect. Genet. Evol.* **2019**, *73*, 159–166. https://doi.org/10.1016/j.meegid.2019.04.020.
28. Techera, C.; Tomás, G.; Panzera, Y.; Banda, A.; Perbolianachis, P.; Pérez, R.; Marandino, A. Development of Real-Time PCR Assays for Single and Simultaneous Detection of Infectious Bursal Disease Virus and Chicken Anemia Virus. *Mol. Cell. Probes* **2019**, *43*, 58–63. https://doi.org/10.1016/j.mcp.2018.11.004.
29. Zierenberg, K.; Nieper, H.; van den Berg, T.P.; Ezeokoli, C.D.; Voss, M.; Müller, H. The VP2 Variable Region of African and German Isolates of Infectious Bursal Disease Virus: Comparison with Very Virulent, "Classical" Virulent, and Attenuated Tissue Culture-Adapted Strains. *Arch. Virol.* **2000**, *145*, 113–125. https://doi.org/10.1007/s007050050009.
30. Zierenberg, K.; Raue, R.; Muller, H. Rapid Identification of "Very Virulent" Strains of Infectious Bursal Disease Virus by Reverse Transcription-Polymerase Chain Reaction Combined with Restriction Enzyme Analysis. *Avian Pathol.* **2001**, *30*, 55–62. https://doi.org/10.1080/03079450020023203.
31. Islam, M.R.; Rahman, S.; Noor, M.; Chowdhury, E.H.; Müller, H. Differentiation of Infectious Bursal Disease Virus (IBDV) Genome Segment B of Very Virulent and Classical Lineage by RT-PCR Amplification and Restriction Enzyme Analysis. *Arch. Virol.* **2012**, *157*, 333–336. https://doi.org/10.1007/s00705-011-1159-9.
32. Katoh, K.; Rozewicki, J.; Yamada, K.D. MAFFT Online Service: Multiple Sequence Alignment, Interactive Sequence Choice and Visualization. *Brief. Bioinform.* **2019**, *20*, 1160–1166. https://doi.org/10.1093/bib/bbx108.
33. Guindon, S.; Dufayard, J.-F.; Lefort, V.; Anisimova, M.; Hordijk, W.; Gascuel, O. New Algorithms and Methods to Estimate Maximum-Likelihood Phylogenies: Assessing the Performance of PhyML 3.0. *Syst. Biol.* **2010**, *59*, 307–321. https://doi.org/10.1093/sysbio/syq010.
34. Letunic, I.; Bork, P. Interactive Tree of Life (iTOL) v6: Recent Updates to the Phylogenetic Tree Display and Annotation Tool. *Nucleic Acids Res.* **2024**, *52*, W78–W82. https://doi.org/10.1093/nar/gkae268.
35. Tamura, K.; Nei, M.; Kumar, S. Prospects for Inferring Very Large Phylogenies by Using the Neighbor-Joining Method. *Proc. Natl. Acad. Sci. USA* **2004**, *101*, 11030–11035. https://doi.org/10.1073/pnas.0404206101.
36. Kumar, S.; Stecher, G.; Suleski, M.; Sanderford, M.; Sharma, S.; Tamura, K. MEGA12: Molecular Evolutionary Genetic Analysis Version 12 for Adaptive and Green Computing. *Mol. Biol. Evol.* **2024**, *41*, msae263. https://doi.org/10.1093/molbev/msae263.
37. Murrell, B.; Wertheim, J.O.; Moola, S.; Weighill, T.; Scheffler, K.; Kosakovsky Pond, S.L. Detecting Individual Sites Subject to Episodic Diversifying Selection. *PLoS Genet.* **2012**, *8*, e1002764. https://doi.org/10.1371/journal.pgen.1002764.
38. Kosakovsky Pond, S.L.; Frost, S.D.W. Not so Different after All: A Comparison of Methods for Detecting Amino Acid Sites under Selection. *Mol. Biol. Evol.* **2005**, *22*, 1208–1222. https://doi.org/10.1093/molbev/msi105.
39. Martin, D.P.; Varsani, A.; Roumagnac, P.; Botha, G.; Maslamoney, S.; Schwab, T.; Kelz, Z.; Kumar, V.; Murrell, B. RDP5: A Computer Program for Analyzing Recombination in, and Removing Signals of Recombination from, Nucleotide Sequence Datasets. *Virus Evol.* **2021**, *7*, veaa087. https://doi.org/10.1093/ve/veaa087.
40. Ikuta, N.; Kipper, D.; Fonseca, A.S.K.; Lunge, V.R. Infectious Bursal Disease Virus Genotypic Diversity from Poultry in Latin America. *Viruses* **2026**, *18*, 746. https://doi.org/10.3390/v18070746.
41. Wyeth, P.J.; Cullen, G.A. Maternally Derived Antibody--Effect on Susceptibility of Chicks to Infectious Bursal Disease. *Avian Pathol.* **1976**, *5*, 253–260. https://doi.org/10.1080/03079457608418194.

42. Wood, G.W.; Muskett, J.C.; Thornton, D.H. The Interaction of Live Vaccine and Maternal Antibody in Protection against Infectious Bursal Disease. *Avian Pathol.* **1981**, *10*, 365–373. https://doi.org/10.1080/03079458108418485.
43. Zhao, S.; Jia, Y.; Han, D.; Ma, H.; Shah, S.Z.A.; Ma, Y.; Teng, K. Influence of the Structural Development of Bursa on the Susceptibility of Chickens to Infectious Bursal Disease Virus. *Poult. Sci.* **2016**, *95*, 2786–2794. https://doi.org/10.3382/ps/pew192.
44. Crespo, R.; Badcoe, L.M.; Williams, C.; Bary, A.I. Inactivation of Infectious Bursal Disease Virus Through Composting of Litter from Poultry Houses. *Avian Dis.* **2016**, *60*, 506–510. https://doi.org/10.1637/11341-120615-ResNote.
45. Voss-Rech, D.; Trevisol, I.M.; Brentano, L.; Silva, V.S.; Rebelatto, R.; Jaenisch, F.R.F.; Okino, C.H.; Mores, M.A.Z.; Coldebella, A.; Botton, S. de A.; et al. Impact of Treatments for Recycled Broiler Litter on the Viability and Infectivity of Microorganisms. *Vet. Microbiol.* **2017**, *203*, 308–314. https://doi.org/10.1016/j.vetmic.2017.03.020.
46. Fahey, K.J.; Crooks, J.K.; Fraser, R.A. Assessment by ELISA of Passively Acquired Protection against Infectious Bursal Disease Virus in Chickens. *Aust. Vet. J.* **1987**, *64*, 203–207. https://doi.org/10.1111/j.1751-0813.1987.tb15182.x.
47. Gallardo, R.A.; Carrasco-Medanic, R.; Zhou, H.; Lyu, S.; Wang, Y.; Woolcock, P.R.; Hoerr, F.J. Effects of Challenge with Very Virulent Infectious Bursal Disease Virus Reassortants in Commercial Chickens. *Avian Dis.* **2014**, *58*, 579–586. https://doi.org/10.1637/10844-040914-Reg.1.
48. Tomás, G.; Marandino, A.; Courtillon, C.; Amelot, M.; Keita, A.; Pikula, A.; Hernández, M.; Hernández, D.; Vagnozzi, A.; Panzera, Y.; et al. Antigenicity, Pathogenicity and Immunosuppressive Effect Caused by a South American Isolate of Infectious Bursal Disease Virus Belonging to the "Distinct" Genetic Lineage. *Avian Pathol.* **2019**, *48*, 245–254. https://doi.org/10.1080/03079457.2019.1572867.
49. Nooruzzaman, M.; Hossain, I.; Rahman, M.M.; Uddin, A.J.; Mustari, A.; Parvin, R.; Chowdhury, E.H.; Islam, M.R. Comparative Pathogenicity of Infectious Bursal Disease Viruses of Three Different Genotypes. *Microb. Pathog.* **2022**, *169*, 105641. https://doi.org/10.1016/j.micpath.2022.105641.
50. Mosad, S.M.; Elsayed, M.M.; Hammad, E.M.; Hendam, B.M.; Ali, H.S.; Eladl, A.H.; Saif, M.A. Genotype Classification and Pathogenicity of Infectious Bursal Disease Virus Circulating in Vaccinated Broiler Chicken Farms. *Vet. Res. Commun.* **2024**, *48*, 3089–3104. https://doi.org/10.1007/s11259-024-10468-z.
51. Pikuła, A.; Lisowska, A.; Jasik, A.; Śmietanka, K. Identification and Assessment of Virulence of a Natural Reassortant of Infectious Bursal Disease Virus. *Vet. Res.* **2018**, *49*, 89. https://doi.org/10.1186/s13567-018-0586-y.
52. Zierenberg, K.; Raue, R.; Nieper, H.; Islam, M.R.; Eterradossi, N.; Toquin, D.; Müller, H. Generation of Serotype 1/Serotype 2 Reassortant Viruses of the Infectious Bursal Disease Virus and Their Investigation In Vitro and In Vivo. *Virus Res.* **2004**, *105*, 23–34. https://doi.org/10.1016/j.virusres.2004.04.009.
53. Nouën, C.L.; Rivallan, G.; Toquin, D.; Darlu, P.; Morin, Y.; Beven, V.; de Boisseson, C.; Cazaban, C.; Comte, S.; Gardin, Y.; et al. Very Virulent Infectious Bursal Disease Virus: Reduced Pathogenicity in a Rare Natural Segment-B-Reassorted Isolate. *J. Gen. Virol.* **2006**, *87*, 209–216. https://doi.org/10.1099/vir.0.81184-0.
54. Schnitzler, D.; Bernstein, F.; Müller, H.; Becht, H. The Genetic Basis for the Antigenicity of the VP2 Protein of the Infectious Bursal Disease Virus. *J. Gen. Virol.* **1993**, *74*, 1563–1571. https://doi.org/10.1099/0022-1317-74-8-1563.
55. Lee, C.-C.; Ko, T.-P.; Chou, C.-C.; Yoshimura, M.; Doong, S.-R.; Wang, M.-Y.; Wang, A.H.-J. Crystal Structure of Infectious Bursal Disease Virus VP2 Subviral Particle at 2.6A Resolution: Implications in Virion Assembly and Immunogenicity. *J. Struct. Biol.* **2006**, *155*, 74–86. https://doi.org/10.1016/j.jsb.2006.02.014.
56. Pikuła, A.; Lisowska, A.; Jasik, A.; Perez, L.J. The Novel Genetic Background of Infectious Bursal Disease Virus Strains Emerging from the Action of Positive Selection. *Viruses* **2021**, *13*, 396. https://doi.org/10.3390/v13030396.
57. Nour, I.; Blakey, J.R.; Alvarez-Narvaez, S.; Mohanty, S.K. Whole Genome Sequencing of Infectious Bursal Disease Viruses Isolated from a Californian Outbreak Unravels the Underlying Virulence Markers and Highlights Positive Selection Incidence. *Viruses* **2023**, *15*, 2044. https://doi.org/10.3390/v15102044.
58. Asfor, A.S.; Reddy, V.R.A.P.; Nazki, S.; Urbaniec, J.; Brodrick, A.J.; Broadbent, A.J. Modeling Infectious Bursal Disease Virus (IBDV) Antigenic Drift In Vitro. *Viruses* **2022**, *15*, 130. https://doi.org/10.3390/v15010130.
59. Gao, H.; Wang, Y.; Gao, L.; Zheng, S.J. Genetic Insight into the Interaction of IBDV with Host-A Clue to the Development of Novel IBDV Vaccines. *Int. J. Mol. Sci.* **2023**, *24*, 8255. https://doi.org/10.3390/ijms24098255.

Disclaimer/Publisher's Note: The statements, opinions and data contained in all publications are solely those of the individual author(s) and contributor(s) and not of MDPI and/or the editor(s). MDPI and/or the editor(s) disclaim responsibility for any injury to people or property resulting from any ideas, methods, instructions or products referred to in the content.